Solid-State Diode-like Chemiluminescence Based on Serial, Immobilized Concentration Gradients in Mixed-Valent Poly[Ru(vbpy)$_3$](PF$_6$)$_2$ Films

Karolyn M. Maness,† Roger H. Terrill,‡ Thomas J. Meyer, Royce W. Murray,* and R. Mark Wightman*

Contribution from the Kenan Laboratories of Chemistry, University of North Carolina, Chapel Hill, North Carolina 27599-3290

Received September 18, 1995. Revised Manuscript Received July 31, 1996[⊗]

Abstract: The electronic conductivity and electrogenerated chemiluminescence (ECL) of thin, electropolymerized films of the fixed-site redox polymer poly[Ru(vbpy)$_3$](PF$_6$)$_2$ (vbpy = 4-vinyl-4′-methyl-2,2′-bipyridine) on Pt interdigitated array electrodes were examined for both solvent-swollen and dry films. In both cases emission arose from *Ru^{2+} produced via the electron-transfer reaction between Ru^{3+} and Ru^{1+} states within the film (Ru = Ru(vbpy)$_3$). Dry films contained fixed concentration gradients of Ru^{3+}, Ru^{2+}, and Ru^{1+} states which were first introduced in an acetonitrile-swollen film via the constant potential oxidation and reduction of Ru^{2+} at opposing IDA fingers. The gradients were then immbolized by drying and cooling the film while retaining the inter-electrode bias (2.6 V). The resulting dried and cooled films responded rapidly to changes in voltage bias and exhibited diode-like characteristics, conducting and emitting light at biases ≥2.6 V and undergoing a reverse bias breakdown current, unassociated with light emission, at ca. −5.5 V. At 0 °C the optimum quantum efficiency of solid-state ECL emission (ϕ_{ECL}) was similar to that in solvent-swollen films: 0.0003 photon/electron. In contrast to the dry films, solvent-swollen films were slow to respond to changes in voltage bias and did not exhibit diode-like behavior.

This paper describes the behavior of a microstructure that exhibits novel diode-like current−voltage and light-emitting behavior in the solid state. The microstructure employs thin (*ca*. 200 nm) solvent-free films of the fixed-site redox conductor poly[Ru(vbpy)$_3$](PF$_6$)$_2$ (vbpy = 4-vinyl-4′-methyl-2,2′-bipyridine) that have been electrochemically deposited on Pt interdigitated array (IDA) electrodes. This and other similar fixed-site redox polymers are not semiconductor materials, but are well-known[1−12] to transport electrons by hopping or self-exchange between donor and acceptor sites. In the solvent swollen state, electrolytic generation of adjacent mixed valent layers containing concentration gradients of Ru^{3+}/Ru^{2+} and Ru^{2+}/Ru^{1+} (Ru = Ru(vbpy)$_3$ and the superscript indicates the formal oxidation state of the complex) (Figure 1) results in light emission termed electrogenerated chemiluminescence (ECL), as a result of reaction between Ru^{3+} and Ru^{1+} states (reaction 1).[13]

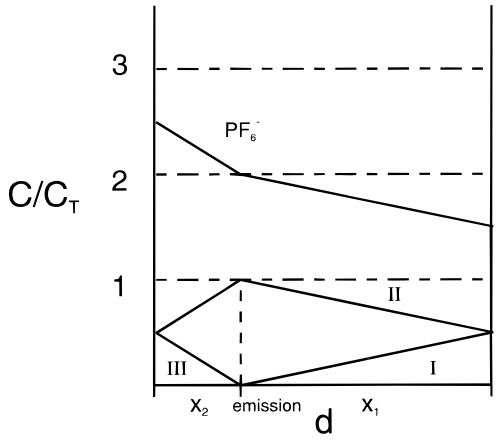

Figure 1. Schematic of the steady-state concentration−distance profiles of Ru(III), Ru(II), and Ru(I) sites and PF$_6^-$ counterions in an acetonitrile swollen poly[Ru(vbpy)$_3$](PF$_6$)$_2$ film deposited on an IDA for an interfinger bias of 2.6 V. The left ordinate represents the anode and the right ordinate represents the cathode for a parallel plate approximation of an interdigitated array electrode. Profiles were determined for $D_{E3+/2+} = 1.9 \pm 0.3 \times 10^{-8}$ and $D_{E2+/1+} = 7.7 \pm 0.2 \times 10^{-8}$ cm^2/s. C_T is the total Ru site concentration in the film, 1.3 M. x_1 and x_2 are the distances from the cathode and anode, respectively.

$$Ru^{1+} + Ru^{3+} \rightarrow {}^*Ru^{2+} + Ru^{2+} \rightarrow 2Ru^{2+} + h\nu \quad (1)$$

When this film is dried (still under the voltage bias), cooled, and examined under various voltage biases, we find that the light intensity varies assymetrically with applied voltage, i.e.,

* To whom correspondence should be addressed.

† Present address: Upjohn CO., Kalamazoo, MI, 49008.

‡ Present address: Department of Chemistry, University of Illinois at Urbana−Champaign, Urbana, IL 61801.

[⊗] Abstract published in *Advance ACS Abstracts,* October 1, 1996.

(1) Pickup, P. G.; Murray, R. W. *J. Am. Chem. Soc.* **1983**, *105*, 4510−4514.

(2) Pickup, P. G.; Kutner, W.; Leidner, C. R.; Murray, R. W. *J. Am. Chem. Soc.* **1984**, *106*, 1991−1998.

(3) Jernigan, J. C.; Chidsey, C. E. D.; Murray, R. W. *J. Am. Chem. Soc.* **1985**, *107*, 2824−2826.

(4) Chidsey, C. E.; Feldman, B. J.; Lundgren, C.; Murray, R. W. *Anal. Chem.* **1986**, *58*, 601−607.

(5) Chidsey, C. E. D.; Murray, R. W. *Science* **1986**, *231*, 25−31.

(6) Jernigan, J. C.; Murray, R. W. *J. Am. Chem. Soc.* **1987**, *109*, 1738−1745.

(7) Jernigan, J. C.; Murray, R. W. *J. Phys. Chem.* **1987**, *91*, 2030−2032.

(8) Jernigan, J. C.; Surridge, N. A.; Zvanut, M. E.; Silver, M.; Murray, R. W. *J. Phys. Chem.* **1989**, *93*, 4620−4627.

(9) Dalton, E. F.; Surridge, N. A.; Jernigan, J. C.; Wilbourn, K. O.; Facci, J. S.; Murray, R. W. *Chem. Phys.* **1990**, *141*, 143−157

(10) Surridge, N. A.; Zvanut, M. E.; Keene, F. R.; Sosnoff, C. S.; Silver, M.; Murray, R. W. *J. Phys. Chem.* **1992**, *96*, 962−970.

(11) Sullivan, M. G.; Murray, R. W. *J. Phys. Chem.* **1994**, *98*, 4343−4351.

(12) Abruna, H. D. *Electroresponsive Molecular and Polymeric Systems*; Skotheim, T., Ed.; Marcell Dekker: New York, 1988; pp 97−171.

(13) Abruna, H. D.; Bard, A. J. *J. Am. Chem. Soc.* **1982**, *104*, 2611−2642.

S0002-7863(95)03185-4 CCC: $12.00 © 1996 American Chemical Society

in a diode-like manner, as does the current. Electrolytically-based I−E diode-like behavior,[5,14−18] ECL[4,19−25] in solutions, and ECL from solvent-contacted polymer films coated on electrodes[26−33] (including[13] poly[$Ru(vbpy)_3$]$(PF_6)_2$) are well-known, but to our knowledge this is the first report of a redox polymer film structure that, once prepared, does not require a net material compositional change to turn forward bias current and light emission on and off. Rather, in the solvent-free state, the Ru^{3+}/Ru^{2+} and Ru^{2+}/Ru^{1+} concentration gradients are fixed in place as a consequence of the immobilization of counterions. ECL via reaction 1 still occurs, but the magnitude and potential bias dependency of the current flow and emission intensity in the dry state are principally governed by and rise with sustained voltage gradients in the redox polymer film, and do not exhibit the limiting current plateaus[3,6−11] that are characteristic of charge transport processes subject to Fick's law transport control.

Electron transport by electron hopping or self-exchange has been extensively investigated for poly[$Ru(vbpy)_3$]$(PF_6)_2$ and analogous fixed-site redox polymer coatings on electrodes. The mixed valent states (e.g., Ru^{3+}/Ru^{2+}) necessary for electron transport are ordinarily generated by electrolysis. Electron transport has been examined in solvent-swollen films,[1−6,9−11] in dry mixed-valent films containing mobile charge-compensating counterions,[3,7,8] in dry mixed-valent films in which the counterions are not mobile,[7−11,35] and most recently in dry, mixed-valent films containing frozen concentration gradients of donor and acceptor sites.[36,37] In dry mixed-valent films containing mobile counterions and sandwiched between two electrodes,[3,7] irrespective of the voltage applied, a limit to the electron transport current is reached when the donor and acceptor concentration gradients electrolytically reach their maximum amplitude. When the film's counterions are not mobile, however, electrolyses that induce further changes in interfacial composition cannot occur and a substantial voltage gradient can be impressed across the film's bulk leading to a rise in electron hopping rates between donor and acceptor without limit[8] as the applied voltage is increased, up to dielectric breakdown. For a given mixed-valent material, we know how[9,11] to reconcile results from these two different modes of supplying free energy to an electron hopping reaction to obtain a common reaction rate constant.

If a gradient of concentration is electrolytically generated and then the counterion's mobility removed, recent results[35] for mixed-valent viologen films with a single concentration gradient (e.g., V^{2+}/V^{1+}) show that the current−voltage behavior of the "frozen gradient" film only modestly differs from that of the same mixed-valent film without a concentration gradient. In comparing currents for applied voltages of the same sign as that forming the concentration gradient ("forward bias") to those for oppositely signed voltage ("reverse bias"), no or only weak diode-like behavior could be seen.

In this work, *two* (serial) sets of concentration gradients, in contacting Ru^{3+}/Ru^{2+} and Ru^{2+}/Ru^{1+} mixed valent layers, are electrolytically introduced into initially all-Ru^{2+} films of poly-[$Ru(vbpy)_3$]$(PF_6)_2$ on IDA electrodes. The electronic and light emissive properties of these gradient-containing films are reported for both solvent-swollen films (ionically conductive) and dried films at lowered temperatures which are not ionically conductive. Examination of the film's ECL under these different conditions allows the electronic and emissive properties of these films to be compared and contrasted for conditions of concentration gradient and voltage gradient driven electron transport.

We should point to the substantial recent interest in the use of semiconducting electroluminescent conjugated polymers for the fabrication of light-emitting diodes.[38−44] This interest arises from the advantages that polymer-based LED's have over conventional inorganic semiconducting materials in their mechanical flexibility, ease of processing, and wide spectral range. In such solid-state polymeric LED's, conduction occurs through delocalized band states with charge (electron/hole) injection accomplished by tunneling at metal contacts.[45] Emission occurs through electron-hole recombinations along the conjugated polymer chains which result in localized excited states. The redox material employed in this paper is qualitatively different from the above semiconducting materials since conduction occurs by electron hopping between well-defined metal complex sites and emission occurs through the bimolecular reaction of neighboring Ru^{3+} and Ru^{1+} states. Thus, the light-emitting and diode-like properties of the present material depend on the existence of built-in concentration gradients of Ru^{3+} and Ru^{1+} states for their existence.

Experimental Section

Chemicals. Acetonitrile (UV grade, Burdick and Jackson) was sparged with N_2 and passed through an activated alumina column prior to solution preparation. Solutions and electropolymerized films were

(14) Denisevich, P.; Willman, K. W.; Murray, R. W. *J. Am. Chem. Soc.* **1981**, *103*, 4727−4737.
(15) Abruna, H. D.; Denisevich, P.; Umana, M.; Meyer, T. J.; Murray, R. W. *J. Am. Chem. Soc.* **1981**, *103*, 1−5.
(16) Pickup, P. G.; Murray, R. W. *J. Electrochem. Soc.* **1984**, *131*, 833−839.
(17) Kittlesen, G. P.; White, H. S.; Wrighton, M. S. *J. Am. Chem. Soc.* **1984**, *106*, 7389−7396.
(18) Paul, E. W.; Ricco, A. J.; Wrighton, M. S. *J. Phys. Chem.* **1985**, *89*, 1441−1447.
(19) Faulkner, L. R. *Int. Rev. Sci., Phys. Chem. Ser. Two* **1975**, *9*, 213−263.
(20) Faulkner, L. R.; Bard, A. J. *Electroanalytical Chemistry*; Bard, A. J., Ed.; Marcel Dekker: New York, 1977; Vol. 10, pp 1−95.
(21) Faulkner, L. R. *Methods Enzymol.* **1978**, *57*, 494−526.
(22) Park, S.; Tryk, D. A. *Rev. Chem. Intermed.* **1981**, *4*, 43−79.
(23) Faulkner, L. R.; Glass, R. S. *Chemical and Biological Generation of Excited States*; Adam, W., Cilento, G.; Academic Press: New York, 1982; pp 191−227.
(24) Gundermann, K. D.; McCapra, F. *Chemiluminescence in Organic Chemistry*; Gundermann, K. D., McCapra, F., Eds.; Springer-Verlag: New York, 1987; pp 130−147.
(25) Knight, A. W.; Greenway, G. M. *Analyst* **1994**, *119*, 879−890.
(26) Rubinstein, I.; Bard, A. J. *J. Am. Chem. Soc.* **1981**, *103*, 5007−5013.
(27) Fan, F.-R. F.; Mau, A.; Bard, A. J. *Chem. Phys. Lett.* **1985**, *116*, 400−404.
(28) Abruna, H. D. *J. Electrochem. Soc.* **1985**, *132*, 842−849.
(29) Zhang, X.; Bard, A. J. *J. Phys. Chem.* **1988**, *92*, 5566−5569.
(30) Miller, C. J.; McCord, P. *Langmuir* **1991**, *7*, 2781−2787.
(31) Obeng, Y. S.; Bard, A. J. *Langmuir* **1991**, *7*, 195−201.
(32) Xu, X.; Bard, A. J. *Langmuir* **1994**, *10*, 2409−2414.
(33) Richter, M. M.; Fan, F. F.; Klavetter, F.; Heeger, A. J.; Bard, A. J. *Chem. Phys. Lett.* **1994**, *226*, 115−120.
(34) Reference deleted in press.
(35) Terrill, R. G.; Sheehan, P. E.; Long, V. C.; Washburn, S.; Murray, R. W. *J. Phys. Chem.* **1994**, *98*, 5127−5134.
(36) Terrill, R. H.; Hatazawa, T.; Murray, R. W. Electron Transport and Frozen Concentration Gradients in a Mixed Valent, Viologen Molten Salt. *J. Phys. Chem.* Accepted for publication.
(37) Terrill, R. H.; Hutchenson, J. E.; Murray, R. W. Frozen Concentration Gradients and Solid State Electron Hopping Transport in a Novel Viologen−Tetraethylene Oxide Copolymer. Manuscript in preparation.
(38) Burroughes, J. H.; Bradley, D. D. C.; Brown, A. R.; Marks, R. N.; Mackay, K.; Friend, R. H. ; Burns, P. L.; Holmes, A. B. *Nature* **1990**, *347*, 539−541.
(39) Gustafsson, G.; Cao, Y.; Treacy, G. M.; Klavetter, F.; Colaneri, N.; Heeger, A. J. *Nature* **1992**, *357*, 477−479.
(40) Burn, P. L.; Kraft, A.; Baigent, D. R.; Bradley, D. D. C.; Brown, A. R.; Friend, R. H.; Gymer, R. W.; Holmes, A. B.; Jackson, R. W. *J. Am. Chem. Soc.* **1993**, *115*, 10117−10124.
(41) Greenham, N. C.; Moratti S. C.; Bradley, D. C.; Friend, R. H.; Holmes, A. B. *Nature* **1993**, *365*, 628−630.
(42) Berggren, M.; Inganas, O.; Gustafsson, G.; Rasmusson, J.; Andersson, M. R.; Hjertberg, T.; Wennerstrom, O. *Nature* **1994**, *372*, 444−446.
(43) Granstrom, M.; Berggren, M.; Inganas, Olle *Science* **1995**, *267*, 1479−1481.
(44) Kido, J.; Kimura, M.; Nagai, K. *Science* **1995**, *267*, 1332−1334.
(45) Parker, I. D. *J. Appl. Phys.* **1994**, *75*, 1656−1666.

prepared in an inert atmosphere glovebox. 9,10-Diphenylanthracene (DPA) and tetra-*n*-butylammonium hexafluorophosphate (Bu_4NPF_6) were recrystallized twice from absolute and 95% ethanol, respectively. $[Ru(vbpy)_3](PF_6)_2$ (vbpy = 4-vinyl-4′-methyl-2,2′-bipyridine) was prepared as described previously.[14] Solid chemicals were dried under reduced pressure at 60 °C for several hours. All chemicals except as noted were reagent grade or better (Aldrich).

Electrodes. Interdigitated array (IDA) electrodes consisting of 100 (n_f) interlocking 3 μm wide, 2 mm long (l), and 0.1 μm thick (h) platinum film fingers separated by 5 μm, generously donated by Nippon Telephone and Telegraph, were patterned on Si/SiO_2 substrates with an insulating Si_3N_4 overlayer surrounding the electrode pattern. Electrodes were cleaned by wiping with an isopropyl alcohol soaked swab, rinsing with isopropyl alcohol, and drying in a N_2 stream, followed by 2 min of exposure to a 200 mT argon plasma.

Polymer Film Preparation. Poly$[Ru(vbpy)_3](PF_6)_2$ films on IDA's were prepared reductively under N_2 by cyclically scanning the potentials of the IDA fingers (shorted together) between 0 and −1.65 V *vs* Ag quasi-reference at 200 mV/s in an electrolyte solution containing 1 mM monomer as described before.[46] Potential control was with a Pine Model RDE4 bipotentiostat and a PAR Model 175 Universal Programmer. The deposited quantity of electroactive polymer, Γ_T, was measured from a slow potential scan $Ru^{3+/2+}$ cyclic voltammogram in 0.1 M Bu_4NPF_6/CH_3CN; conversion to film thickness was based on a 1.3 M site concentration obtained ellipsometrically for a structurally similar polymer.[47] A typical IDA film thickness was 200 nm; larger thicknesses were avoided owing to problems with adhesion to the IDA.

Cell for ECL Observations. IDA electrodes were secured on a Teflon holder in a manner ensuring reproducible positioning in front of the photomultiplier tube. The cell, made from 1 in. i.d. glass tubing, had three Kontes PTFE valves for control of N_2 flow, exposure to vacuum, and addition or removal of electrolyte solution, and a cell top with an O-ring seal and tungsten wire feedthroughs for electrical connection to the IDA. The auxiliary electrode was a Pt mesh and the reference was Ag/0.01 M $AgBF_4$/0.1 M Bu_4NBF_4/CH_3CN (310 mV *vs* SSCE) connected through a Vycor frit. Both the auxiliary and reference electrodes were positioned below the solution control valve. A photomultiplier tube housing (Instruments SA, Inc.) faced the IDA through a threaded Al adapter glued to the side of the cell.

Preparation of and Current−Voltage Measurements in Dry, Fixed-Concentration, Gradient-Containing Films. The ECL cell described above was carefully dried by heating under a flow of dry N_2. The poly$[(Ru(vbpy)_3](PF_6)_2$ coated IDA's were then placed in the cell, and the cell was again purged with dry N_2 prior to solution contact. Solutions of 0.1 M Bu_4NPF_6/CH_3CN were prepared in a N_2 glovebox and transferred to the cell in a gas-tight syringe under positive N_2 pressure.

Serial concentration gradients of Ru^{3+}/Ru^{2+} and Ru^{2+}/Ru^{1+} were generated in the film by independently controlling the potentials (using a Pine Model RDE4 bipotentiostat) of the two IDA finger sets at the formal potentials of the $Ru^{3+/2+}$ (0.94 V *vs* Ag/Ag^+) and $Ru^{2+/1+}$ (−1.66 V *vs* Ag/Ag^+) couples until steady-state currents were attained. The electrolyte solution was then withdrawn from the main cell compartment into the reference/auxiliary side compartment; this preserves potential control of the 2.6 V interfinger voltage bias (E_{bias}). The main compartment was then sealed, purged with N_2 for 3 min, and evacuated for an additional 3 min to dry the films. Previous experience with these 200 nm thick films indicates that drying occurs rapidly.[1−7] The interfinger bias is maintained at all times both during and after the drying process to preserve the electrolytically generated concentration gradients.

To reduce the mobility of the PF_6^- counterions beyond that achieved from drying alone, films were cooled with a N_2 stream chilled by liquid N_2 and heated to a controlled temperature using the output of an Omega CN76000 temperature controller. The controlling thermocouple (T-type) was located adjacent to the IDA electrode.

The current−voltage responses of the dry concentration gradient containing films were examined by stepping and sweeping the potential bias applied between the IDA finger sets. Voltage sweeps and steps were provided by a Datel 412 analog IO board in an IBM PC compatible microcomputer employing software of local design. For biases greater than ±5 V, a Kepco B0P100−1M bipolar operational power supply (10×, ±100 V) amplifier was placed in series with the smaller amplitude voltage waveforms.

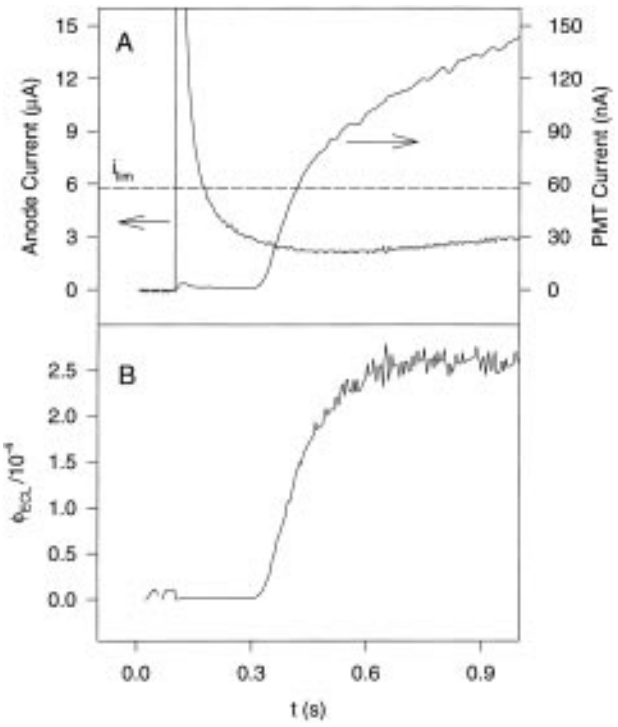

Figure 2. Time course of current, light emission, and quantum efficiency during electrogenerated chemiluminescence for a 200 nm thick poly$[Ru(vbpy)_3](PF_6)_2$ film immersed in a solution of 0.1 M Bu_4NPF_6/acetonitrile upon simultaneous application of $E^{o\prime}_{3+/2+}$ and $E^{o\prime}_{2+/1+}$ ($\Delta E^{o\prime} = 2.6$ V) to the opposing fingers of the IDA at $t = 0.1$ s. $E^{o\prime}_{3+/2+} = 0.94$ V and $E^{o\prime}_{2+/1+} = -1.66$ V *vs* Ag/Ag^+. Panel A: Current at IDA finger set potentiostated at +0.94 V and PMT current; dashed line is the steady state current reached in 10 s. Panel B: ECL quantum efficiency. PMT currents here and in the following figures are calibrated as described in the Experimental Section.

Measurement of Electrogenerated Chemiluminescence. ECL emission was measured using a Hamamatsu R928 photomultiplier tube (PMT) operated at −600 V. The Faraday cage surrounding the ECL cell was covered with black felt to block ambient light. The PMT current was measured using a Stanford Research Systems Model SR570 Low-Noise Current Preamplifier and recorded on a Nicolet 310 digital oscilloscope, strip chart recorder, or a Datel 412 IO board in an IBM PC compatible microcomputer using locally written software.

The ECL efficiency, ϕ_{ECL}, is defined as the number of emitted photons per electron flowing per unit time. The PMT current scale was calibrated with the ECL emission from a 10 mM diphenylanthracene (DPA) solution in 0.1 M Bu_4NPF_6/50:50 (v:v) CH_3CN:toluene, which has a quantum efficiency of 0.064 ± 0.005.[48] The intensity measurements were corrected for differences in PMT sensitivity at the wavelengths of maximum emission (685 nm, poly$[Ru(vbpy)_3](PF_6)_2$; 425 nm, DPA) using the manufacturer's specifications.

Results

Electrolytic ECL Production in Solvent-Swollen Films. Figure 2 illustrates the typical time course of current and light emission observed from a poly$[Ru(vbpy)_3](PF_6)_2$ film immersed in an electrolyte solution after simultaneous application of the formal potentials of the $Ru^{3+/2+}$ and $Ru^{2+/1+}$ couples to the two IDA finger sets.[49] In all experiments in solution, the potentials

(46) Denisevich, P.; Abruna, H. D.; Leidner, C. R.; Meyer, T. J.; Murray, R. W. *Inorg. Chem.* **1982**, *21*, 2153−2161.

(47) McCarley, R. L.; Thomas, R. E.; Irene, E. A.; Murray, R. W. *J. Electrochem. Soc.* **1990**, *137*, 1485−1490.

(48) Maness, K. M.; Bartelt, J. E.; Wightman, R. M. *J. Phys. Chem.* **1994**, *98*, 3993−3998.

(49) These formal potentials were determined prior to applying the potential steps from the average of the anodic and cathodic voltammetric peak potentials obtained at a scan rate of 100 mV/s.

applied to the IDA fingers were versus a separate reference electrode. The current shown in Figure 2A arises from the $Ru^{3+/2+}$ conversion at one of the finger sets. Following an initial decaying current transient for electrolysis of polymer atop the fingers and in the gap, the current is subsequently seen to rise to a steady state value within ca. 10 s (not shown).[50] Light emission ensued typically ~200 ms after the potential step and also approached steady state. After about 500 ms, the increase in light emission intensity closely tracked that of the current, and the emission quantum efficiency, ϕ_{ECL}, stabilized (Figure 2B). The response was the same if the potentials applied to the two finger sets were reversed.

The current minimum and approach toward steady state[50] in Figure 2A reflects a complex evolution of Ru^{3+}/Ru^{2+} and Ru^{2+}/Ru^{1+} concentration gradients toward the linear ones illustrated in Figure 1, and is consistent with other descriptions of redox polymers deposited between contacting electrodes.[3,6,7,9,11] The delay between the application of the potential steps and the onset of ECL emission (Figure 2B) reflects the time necessary to electrolyze Ru^{2+} to Ru^{1+} and Ru^{3+} and the time required for these latter valence states to travel by electron hopping to the point within the interelectrode gap where they meet and react. An analogous delay is observed with double-band microelectrodes for ECL produced from two freely diffusing species in solution.[48,51]

Increasing the potential difference applied between the IDA fingers beyond the formal potentials of the $Ru^{3+/2+}$ and $Ru^{2+/1+}$ couples initially produced larger currents and light emission but little change in ϕ_{ECL}. However, application of potential differences sufficiently large to generate Ru^0 sites in the film led to currents and emission which decayed with time yielding a ϕ_{ECL} half its original value. The decay and decreased ϕ_{ECL} can be attributed to a chemical instability of Ru^0. Similar instability of $[Ru(bpy)_3]^0$ has been observed in solution.[52,53] Since the production of Ru^0 occurs at potentials very close to those for prodution of Ru^{1+}, to avoid such decay, all following experiments employed steps to the formal potentials of the $Ru^{3+/2+}$ and $Ru^{2+/1+}$ couples. Application of the formal potentials also has the added benefit of increasing the conductivity of the film close to the electrodes allowing for efficient movement of charge from the electrode/film interface into the emission region.

The ECL quantum efficiency, ϕ_{ECL}, observed for solvent-swollen films on IDA's varied significantly with each film prepared with ECL efficiencies ranging over two orders of magnitude. The maximum observed efficiency was *ca.* 0.00025, or 200 times less than that for $[Ru(bpy)_3]^{2+}$ monomer in acetonitrile ($\phi_{ECL} = 0.05$ at 25 °C).[54] The reduced ϕ_{ECL} in the polymeric film reflects the presence of additional nonradiative pathways for excited state relaxation in the film vs. solution. A major factor is the existence of excited state/ground state interactions in the highly concentrated (1.3 M) film. The resulting electronic coupling decreases the excited state/ground state energy gap, increasing nonradiative decay.[55] This nonradiative decay accounts for the low emission intensities observed for these films. Similarly low intensities have been observed for films of polymerized $Ru(bpz)_3^{2+}$ (bpz = 2,2′-bipyrazine) into which $Ru(bpy)_3^{2+}$ has been incorporated.[56]

During a 1-h observation the ECL emission intensity and current flow through the film were seen to decay concurrently by 57% and 50%, respectively. This is a much improved stability over that reported in a previous ECL study of this polymer film by Abruna and Bard, in which the emission completely ceased after 20 min.[13] In that study ECL was generated by alternate oxidation and reduction of the film (AC-ECL). Similar AC-ECL studies of these films in our laboratory have shown a similarly short duration of ECL emission (data not shown). Examination of films following AC-ECL revealed a loss of polymer film from the electrode surface. During AC-ECL net changes in film oxidation state require the repeated movement of charge compensating ions into and out of the film. This counterion movement may lead to the differential swelling of the polymer film, compromising film/electrode adhesion. In the present work, however, the use of constant applied potentials removes the necessity of counterion movement during ECL generation.

Measurement of Electron Diffusion in Solvent Swollen Films. Electron transport rates in redox polymeric films are often parametrized as electron diffusion coefficients, D_E, which reflect the dynamics of electron hopping or self exchange within the films.[5,9,57,58] In the present case, $D_{E3+/2+}$ and $D_{E2+/1+}$ for the $Ru^{3+/2+}$ and $Ru^{2+/1+}$ couples, respectively, determine the film's electronic conductivity and also the position of the emitting region within the interelectrode gap.[59] The latter is important because close proximity to the metal finger electrodes could potentially evoke quenching of ECL emission[60−64] and lower the measured ECL quantum efficiency.

$D_{E3+/2+}$ and $D_{E2+/1+}$ were determined (independently of the ECL measurements) through the use of an electrochemical time-of-flight technique,[65−67] and also from steady-state collector−generator currents.[4] The results, $D_{E3+/2+} = 1.9 \pm 0.3 \times 10^{-8}$ cm^2/s and $D_{E2+/1+} = 7.7 \pm 0.2 \times 10^{-8}$ cm^2/s, and their ratio, 4.1, agree with reported values for this and similar redox polymers.[2,4,46] Based on these values, the emissive region can be calculated[59] to be *ca.* 1 μm away from the anode, a distance sufficiently great that quenching of the emissive $^*Ru^{2+}$ excited state due to the proximity of the electrode surface should be unimportant.[30−32]

(50) The minima observed in the current is likely the result of a change in polymer conductance during electrolysis. This change arises from the necessary rearrangement of counterions during the course of establishing the concentration gradients illustrated in Figure 1.

(51) Amatore, C.; Fosset, B.; Maness, K. M.; Wightman, R. M. *Anal. Chem.* **1993**, *65*, 2311−2316.
(52) Luttmer, J. D.; Bard, A. J. *J. Phys. Chem.* **1981**, *85*, 1155−1159.
(53) Glass, R. S.; Faulkner, L. R. *J. Phys. Chem.* **1981**, *85*, 1160−1165.
(54) Wallace, W. L.; Bard, A. J. *J. Phys. Chem.* **1979**, *83*, 1350−1357.
(55) Gould, S.; Guadalope, A.; Meyer, T. J. Unpublished results.
(56) Ghosh, P. K.; Bard, A. J. *J. Electroanal. Chem.* **1984**, *169*, 113−128.
(57) Surridge, N. A.; Jernigan, J. C.; Dalton, E. F.; Buck, R. P.; Watanabe, M.; Zhang, H.; Pinkerton, M.; Wooster, T. T.; Longmire, M. L.; Facci, J. S.; Murray, R. W. *Faraday Discuss. Chem. Soc.* **1989**, *88*, 1−17.
(58) Majda, Marcin *Molecular Design of Electrode Surfaces*; Murray, R. W., Ed.; John Wiley & Sons, Inc.: New York, 1992; pp 159−206.

(59) The location of the emissive region within the interelectrode gap is determined by the relative rates of charge transport within the regions of the film containing the $Ru^{3+/2+}$ and $Ru^{1+/0}$ concentration gradients and dictated by the products of the diffusion coefficients, $D_e^{3+/2+}$ and $D_e^{2+/1+}$, and the concentration gradients $\Delta[Ru^{2+}]/\Delta x$. Since at steady-state the fluxes of charge down the Ru^{3+} and Ru^{1+} gradients are equal, one can solve Fick's first law for the distance over which the concentration gradient of the Ru^{1+} species extends (x_1) (Figure 1):

$$x_1 = \frac{(dD_e^{2+/1+})}{(D_e^{3+/2+} + D_e^{2+/1+})}$$

where d is the interelectrode gap width (5 μm) and x_1 is the distance of the emissive region from the electrode generating the Ru^{+1} species.

(60) Waldeck, D. H.; Alivisatos, A. P.; Harris, C. B. *Surf. Sci.* **1985**, *158*, 103−115.
(61) Chance, R. R.; Prock. A.; Silbey, R. *J. Chem. Phys.* **1974**, *60*, 2744−2748.
(62) Chance, R. R.; Miller, A. H.; Prock, A.; Silbey, R. *Chem. Phys. Lett.* **1975**, *33*, 590−592.
(63) Kuhn, H. *J. Chem. Phys.* **1970**, *53*, 101−108.
(64) Chance, R. R.; Prock, A.; Silbey, R. *Adv. Chem. Phys.* **1978**, *37*, 1−65.
(65) Feldman, B. J.; Feldberg, S. W.; Murray, R. W. *J. Phys. Chem.* **1987**, *91*, 6558−6560.
(66) Cammarata, V.; Talham, D. R.; Crooks, R. M.; Wrighton, M. S. *J. Phys. Chem.* **1990**, *94*, 2680−2684.
(67) Licht, S.; Cammarat, V.; Wrighton, M. S. *J. Phys. Chem.* **1990**, *94*, 6133−6140.

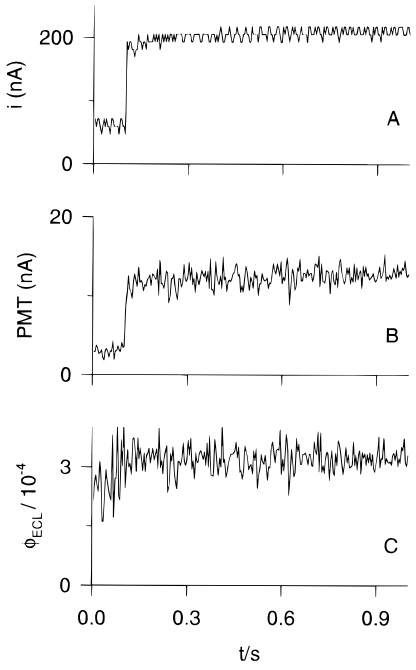

Figure 3. Panel A: Current. Panel B: Light emission as PMT current. Panel C: Quantum efficiency, for a +1 V forward bias voltage step at $t = 0.1$ s from the original interfinger bias of +2.6 V for a dry (0 °C) film containing serial concentration gradients of $Ru^{3+/2+}$ and $Ru^{2+/1+}$. The film is the same as used in Figure 2. The initial current of ca. 70 nA shown in Panel A is less than that in Figure 2A, since the film is dried and cooled.

ECL in Dry Films Containing Frozen Concentration Gradients. Although the ECL observed from both solvent swollen and dry films originates from reaction 1, the voltage and time dependencies of the emission, and the current flow, differed greatly for the two conditions. To examine ECL in dry concentration gradient-containing films, serial gradients in adjacent Ru^{3+}/Ru^{+2} and Ru^{+2}/Ru^{+1} mixed valent layers were generated by the electrolytic process described above and were frozen into place by carefully drying and then cooling the films while maintaining the applied 2.6 V voltage bias. Although the formal potentials of the couples may change during the drying process,[3] current flow and light emission continued during this process indicating that the concentration gradients persist in a form similar to that predicted in Figure 1. Indeed, qualitatively similar behavior was obtained when the films were formed under larger bias although the decreased stability of the solvent swollen film under these conditions (vide supra) prevented more detailed investigation.

Large increases in both current and emission intensity occurred when the voltage bias applied to the dried, cooled (0 °C) film was stepped from +2.6 to +3.6 V (Figure 3A,B). The current and light emission were tightly correlated, yielding a quantum efficiency which increased slightly upon potential application and then remained constant (curve C), In contrast to the results obtained from solvent-swollen films (Figure 2), the response shown in Figure 3 was quite fast (≤ms), and stepping the applied bias back to +2.6 V restored the original current and emission levels just as quickly.

The response of the same film to a ±25 V, 100 V/s voltage sweep about the +2.6 V bias clearly reveals the diode-like character of both current flow and light emission (Figure 4). For forward-bias voltages, the current and conductance (the $i-E$ slope in Figure 4A) increased with increasing voltage bias as has been previously described for electron hopping conductors.[9] (Here forward bias is signed positive and refers to voltages more positive than +2.6 V, while reverse-bias voltages are those less positive than +2.6 V.) Typical forward bias conductivities

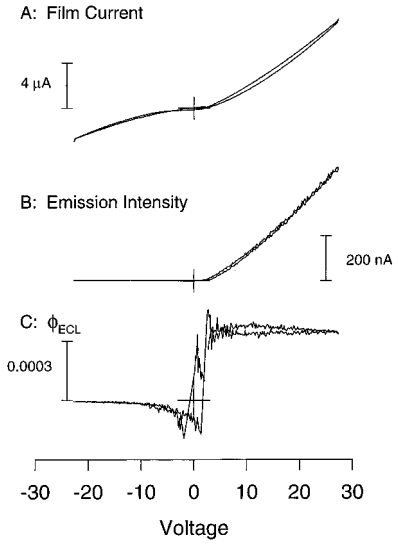

Figure 4. Panel A: Current. Panel B: Light emission as PMT current. Panel C: Quantum efficiency during a 100 V/s, ±25 V voltage sweep centered around an interfinger bias of +2.6 V. The cross hairs represent the 0,0 point on a given plot. The dry (0 °C) poly[$Ru(vbpy)_3$]$(PF_6)_2$ film is identical to that in Figure 3.

ranged from 0.3 to $3 \times 10^{-6}\ \Omega^{-1}\ cm^{-1}$.[68] As with the potential step results (Figure 3B), light emission (Figure 4B) closely tracked the current, leading to a ϕ_{ECL} (Figure 4C) that was remarkably independent of the forward-bias voltage.[69]

For bias voltages less positive (i.e., reverse) than +2.6 V, however, the film current and conductance decreased and no light emission was observed. For reverse bias voltages between *ca.* +2.6 and *ca.* −5.5 V, the film current and conductance were especially attenuated with, in this case, a ca. 15-fold decrease in conductance relative to forward bias (Figure 4A). In observations on several film preparations, film conductance was found to decrease by 10- to 100-fold in this voltage window. For reverse-bias voltages more negative than *ca.* −5.5 V, however, an increase in current was again observed with the reverse-bias conductance only *ca.* 2.5-fold lower than that under forward-bias (Figure 4A). The reverse-bias voltage at which this apparent breakdown in diode-like behavior occurs varied from film to film. Light emission never accompanied the breakdown current, clearly demonstrating that reverse-bias currents are not the result of electrolytic inversion of concentration gradients as would occur in an ionically conductive film.[1−3,6,8]

The diode-like current−voltage characteristics of Figure 4A have not been previously reported in dry, uniformly mixed-valent redox phases or for dry redox films containing a single set (a single redox couple) of frozen concentration gradients.[36,37] They are *formally* reminiscent of a electronic diode with a large forward bias conductance for voltages >2.6 V, low conductance for voltages between 2.6 and ∼−5.5 V, and a large breakdown conductance for voltages more negative than −5.5 V. The observed ratios of forward to reverse bias conductances of 10−100 are comparable to those reported for semiconductor based diodes (>25).

ECL Efficiency and Conductance vs. Temperature in Dry Concentration Gradient Containing Films. The temperature

(68) Assuming a parallel plate polymer sandwich approximation for the films deposited on IDA's, conductance was converted to conductivity by multiplying by the geometric factor, d/A, where d is the interelectrode gap distance of 5 μm, and A is the area of the parallel plate polymer sandwich, $A = (n_f - 1) \times l \times h$. Here l is the length of the IDA Pt finger, h is the finger height, and n_f are the number of fingers.

(69) For a ±25 V, 100 V/s sweep applied to a dry all Ru^{2+} film containing no valence state concentration gradients very little current and no emission was observed.

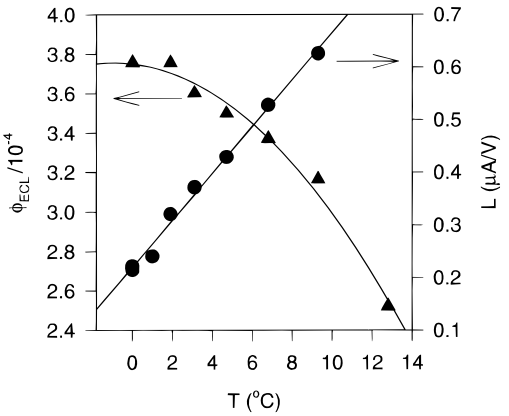

Figure 5. Temperature dependence of average forward bias conductance (●) and ϕ_{ECL} (▲), for a dry film, during the forward bias branch of a 100 V/s, ±10 V sweep recorded while cooling the sample with flowing N_2. The film is the same as used in Figure 4.

dependence of ϕ_{ECL} and conductance of dried gradient-containing films is shown in Figure 5. These data were obtained with periodic ±10 V sweeps around +2.6 V while the electrochemical cell was cooled over the temperature range shown. Figure 5 shows that ϕ_{ECL} and forward-bias conductances increased by 50% and declined by 70%, respectively, over the 13 °C temperature interval.

The observed increase in ECL efficiency with decreasing temperature is consistent with previous ECL studies of $[Ru(bpy)_3]^{2+}$ in solution,[53,70] where ϕ_{ECL} increased by 130% between 25 and 0 °C, due to a decrease in the rate of nonradiative decay of the excited state.[71] The observed decrease in conductance with decreasing temperature is expected for thermally activated electron hopping in a mixed-valent material.[7,8]

Stability of Concentration Gradients in Dry Films. Since light emission from the dry films depends upon reaction 1, the emission must also depend upon the presence and stability of the frozen $Ru^{3+/2+}$ and $Ru^{2+/1+}$ concentration gradients as well as the chemical stabilities of the Ru^{3+} and Ru^{1+} species themselves. To probe these stabilities, ECL of dry concentration gradient-containing films was examined as a function of time, resting bias potential, and potential sweeps.

Figure 6 shows forward-bias conductance and ECL quantum efficiency, ϕ_{ECL}, of a dry (0 °C) concentration gradient-containing film measured with periodic, repeated ±25 V, 100 V/s voltage sweeps as described in the figure legend. (This film was one of a number that emitted with lower efficiency than in preceding figures.) In Panel A, where the voltage bias was held at +2.6 V during the resting intervals between voltage sweeps, the ϕ_{ECL} recorded during the voltage sweep (as in Figure 4C) remained relatively constant over a 1500-s period, decaying by only *ca*. 5%. Over this same period, the forward bias conductance decayed slightly with each successive sweep, recovering somewhat during the periodic longer resting periods to yield an overall decay of 50%. After a 26-min intermission, the film was biased at 0 V (i.e., the IDA was shorted) between periodic voltage sweeps. This caused severe decays in both ϕ_{ECL} (70%) and the forward-bias conductance (80%) over a 1500-s period (Figure 6, Panel B).[72] In Panel C, a +2.6 V resting bias was again used between sweeps, and forward-bias

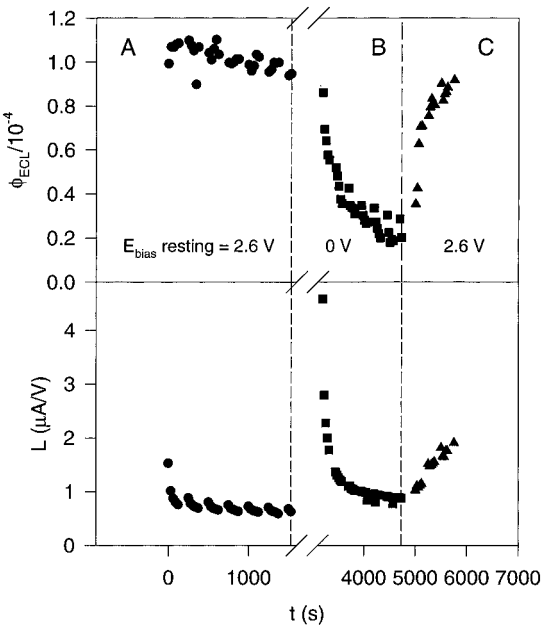

Figure 6. Average forward bias conductance (bottom) and ϕ_{ECL} (top) versus time for a dry film at 0 °C during the forward bias branch of repeated ±25 V, 100 V/s sweeps as a function of time. The bias applied to the film in the time interval between sweeps is 2.6 V (the original bias) for parts A and C and 0 V for part B. Sweeps are recorded every 30 s, with a 130 s delay after every 5th sweep. During the 26-min interval between recording parts A and B, two potential steps (duration, 1 and 5 s; ±5 V around 2.6 V) and three potential sweeps (±25 V around 2.6 V; 100 V/s) were performed.

conductance and ϕ_{ECL} increased with time, the former nearly recovering its initial value in Panel B.

The stability of ϕ_{ECL} during Figure 6A indicates good *chemical* stability of the solvent free films at 0 °C, relative to that of films wetted by solvent (*vide supra*) where the emission efficiency decreased by 25% over the same time period. The other effects seen in Figure 6 indicate that the basis of ECL emission and trans-gap electron transport, i.e., the mixed-valent layers of $Ru^{3+/2+}$ and $Ru^{2+/1+}$ with their frozen concentration gradients can be degraded by repeated (Figure 6A) or prolonged (Figure 6B) excursions into reverse voltage bias. In particular, the decay in ϕ_{ECL} and conductance in Figure 6B, with a 0 V resting voltage bias, reflects a relaxation of the concentration gradients and decrease of Ru^{3+} and Ru^{1+} population in the film. This must originate from a finite ionic mobility of the film's PF_6^- counterions even at 0 °C that makes itself evident on the long observational time scales of Figure 6.[7] That ϕ_{ECL} does not decay entirely shows that relaxation of the concentration gradients is quite slow at 0 °C. The relaxation can be (also slowly) reversed as shown by Figure 6C. The small changes in ϕ_{ECL} and conductance observed in Figure 6A may result simply from the large voltage sweep excursions into reverse bias and not from chemical degradation.

Discussion

The results presented here demonstrate that dry, mixed-valent redox polymers can exhibit diode-like properties in current−voltage behavior and light emission. It should be emphasized that, while these properties are evoked by electrolytic fabrication of $Ru^{3+/2+}$ and $Ru^{2+/1+}$ concentration gradients in the poly$[Ru(vbpy)_3](PF_6)_2$ film, they do not themselves require net interfacial compositional changes for their onset upon application of a potential. Fixed concentration gradients were established by immobilization of counterions by drying and cooling the polymeric films; in principle other counterion immobilization tactics should be possible. The lack of interfacial compositional

(70) Itoh, K.; Honda, K. *Chem. Lett.* **1979**, 99−102.
(71) Van Houten, J.; Watts, R. J. *J. Am. Chem. Soc.* **1976**, *98*, 4853−4858.
(72) The elevation of conductance appearing at the beginning of the second sweep series *may* be an artifact of the 26-min interval between these experiments, during which time 2 potential steps (duration, 1 and 5 s; ±5 V around 2.6 V) and 3 potential sweeps (±25 V around 2.6 V; 100 V/s) were performed.

change results in a microstructure that rapidly responds to changes in voltage unlike traditional electrochemical cells in which mass transport limits response times. We refer to the observed electronic and emissive properties as diode-*like* to emphasize that while the behavior has formal similarity to semiconductor-based microstructures, the poly[Ru(vbpy)$_3$](PF$_6$)$_2$ film is not a semiconductor but conducts by facile electron hopping between electronically well-defined and localized states.

The essential properties exhibited by dry poly[Ru(vbpy)$_3$](PF$_6$)$_2$ films containing fixed concentration gradients of Ru^{3+}/Ru^{2+} and Ru^{2+}/Ru^{1+} in adjacent mixed valent layers include diode-like current and light rectification, fast response times to changes in voltage bias, large operating voltages (±25 V), and an absence of forward-bias limiting currents (out to +25 V). These properties contrast with those exhibited by solvent-swollen films of the same redox material where no current and light rectification are seen, response times are slow, operating voltages are limited by film and solvent electrolysis, and limiting currents exist. The differences in the general electronic properties (i.e. response times, limiting currents and operational voltages) of the above two types of films can be understood through a consideration of the different driving forces for electron hopping which are operative in each case. However, it is the presence of the two sets of serial *frozen* concentration gradients that provides the origin of the diode-like current and light-emitting properties of the dry mixed-valent film since-solvent swollen films which do not contain frozen gradients[36,37] and dry redox polymers which contain only one set of frozen concentration gradients do not exhibit diode-like behavior.

To understand the differences in the general electronic properties of dry and solvent-swollen films first consider how a solvent-swollen film responds to changes in potential bias. Counterions are mobile in solvent-swollen poly[Ru(vbpy)$_3$](PF$_6$)$_2$ films so that application of any potential bias leads to electrolytic adjustment of interfacial and bulk Ru^{3+}, Ru^{2+}, and Ru^{1+} concentrations, with concurrent redistribution of the PF_6^- counterion population in the film. Electron transport is then governed by the magnitude of the redox concentration gradients formed and the values of the D_E's. The former reaches a limiting value and in turn limits the current and light emission. Any adjustments in the concentration gradients are subject to the relatively slow time constant of counterion redistribution.[2,14−16] Ionic mobility also allows reversal of the direction of any concentration gradients upon voltage bias reversal. Thus, rectification effects are not seen.

In contrast, in mixed-valent films with immobile ions, with the application of a voltage bias, electron transport is driven by the voltage gradient rather than by a concentration gradient of redox sites. The absence of a requirement for macroscopic ionic redistributions to evoke electron transport means that both electrical and light emissive responses are much faster. This is seen in the present work in the comparison of Figure 3 with Figure 2, and in the absence of hysteresis in the current−voltage curves in Figure 4A. At a nuclear level charge redistribution occurs to allow reaction 1 to proceed under forward bias. However, because of the lack of ionic movement this electronic redistribution is rapid leading to the observed rapid responses. The reason for increases in intensity of light emission under increasing forward bias is simply an electrical field-controlled rate of electron hopping through the mixed-valent layers that supply Ru^{3+} and Ru^{1+} states to the emitting zone. The analysis of currents in this situation, which increase with voltage bias and do not exhibit limiting values, has been described in several previous papers.[8−11]

The origin of the diode-like behavior of the current and light emission displayed in Figure 4 can be understood through a consideration of the three distinct regions present in the dry mixed-valent film and the role these regions play in forward and reverse bias. As shown in Figure 7, top, in the region of the film adjacent to the IDA finger set which served as the anode during electrolytic formation of the concentration gradients, both Ru^{2+} and Ru^{3+} sites are present, and this region of the film is electronically conductive via electron hopping from Ru^{2+} sites (electron donors) to Ru^{3+} sites (electron acceptors). A corresponding conductive region exists adjacent to the cathode with Ru^{1+} (electron donor) and Ru^{2+} (electron acceptor) sites. At the boundary or junction between these two mixed-valent regions is the emissive zone where conductance proceeds via the electron-transfer reaction between Ru^{1+} and Ru^{3+} (reaction 1).[73] Under a forward voltage bias equal to or larger than 2.6 V, electrons flow through the film in a manner that equates to the transport of Ru^{1+} and Ru^{3+} states toward each other followed by their reaction, excited state emission, and generation of Ru^{2+} states which are transported away from the emission zone.

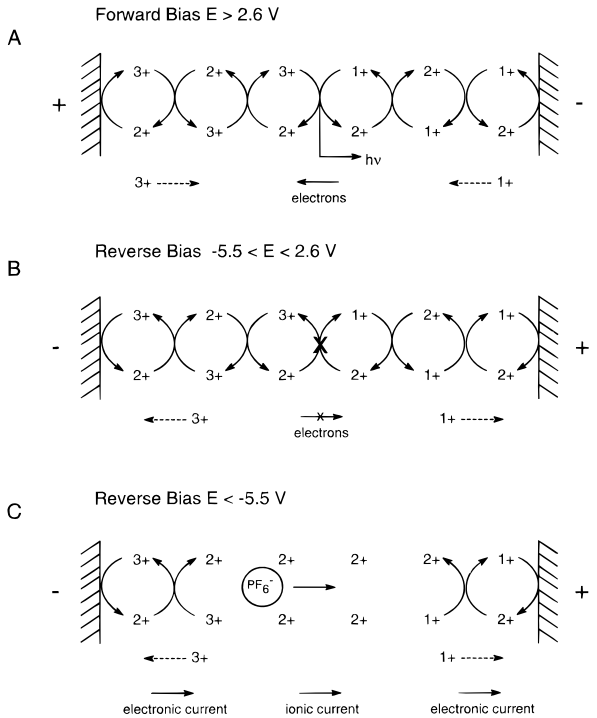

Figure 7. Cartoon depicting the bimolecular hopping transport of electrons (curved arrows) between Ru^{2+} and Ru^{3+} sites (left) and Ru^{1+} and Ru^{2+} sites (right). Panel A (top) shows the forward-bias condition. The dashed arrows indicate the *effective* direction of propagation of Ru^{3+} and Ru^{1+} states toward the emissive boundary region where an electron transfer occurs between Ru^{1+} and Ru^{3+} (comproportionation). Electrons thus hop from right to left through the film. Panel B (middle) shows the reverse voltage bias condition. The direction of electron propagation is reversible in the 3+/2+ and 2+/1+ mixed-valent regions to the left and right of the emissive boundary region, but in this region electron flow is reduced because of the highly unfavorable energetics of the Ru^{2+} disproportionation ($\Delta E \approx -2.6$ V). Panel C, bottom, depicts the proposed breakdown mechanism under reverse bias. Electric fields accumulate in the resistive comproportionation region and force ion movement. This in turn allows the electrolytic conversion of Ru^{1+} and Ru^{3+} to Ru^{2+}.

It is worth re-emphasizing at this point that the quantum efficiency of reaction 1 is roughly the same, ca. 3×10^{-4}, for solvent-wetted room temperature and for dried 0 °C films. This

(73) Given that the ion-annihilation rate for Ru(bpy)$_3^{2+}$ in acetonitrile is diffusion controlled (Collinson, M. M.; Wightman, R. M.; Pastore, P. *J. Phys. Chem.* **1994**, *98*, 11942−11947), it may be assumed that the electron transfer rate for the disproportionation of Ru^{1+} and Ru^{3+} in the film is sufficiently fast as to not limit the overall charge transport rate through the film.

result implies that drying of the films does not aggravate the non-radiative losses that lead to the low quantum efficiency, and that the roughly 10^2-fold decrease in emission intensity upon drying and cooling (compare Figures 2 and 3) is substantially a thermal effect and not a consequence of the drying itself.

For reverse-bias voltages, the driving force is for transport of Ru^{2+} states toward the boundary between the mixed-valent layer and Ru^{1+} and Ru^{3+} states *away from that boundary*. For this to be accomplished, reaction 1 must be driven in the opposite direction, and since this is a highly unfavorable process (short of accumulation of a sufficiently large voltage drop over the boundary region) current flow does not occur. For analogous reasons, light emission does not occur since Ru^{1+} and Ru^{3+} states are driven apart, not together. Reverse bias leads, in effect, to accumulation of Ru^{2+} states and depletion of Ru^{3+} and Ru^{1+} states in the boundary region (Figure 7, middle). Since hopping electron transport is a bimolecular process, requiring both electron donor and acceptor, the depletion of Ru^{3+} and Ru^{1+} in the boundary region makes it less electronically conductive. This process is formally analogous to the majority carrier depletion experienced by a semiconductor p−n junction under reverse bias. The combination of the unfavorable direction of reaction 1 and the presence of the insulating boundary region serves as the proposed root of the diode-like current−voltage behavior.

That the mixed-valent layer boundary region is depleted in Ru^{3+} and Ru^{1+} states and thus resistive also leads under larger reverse bias voltages to the accumulation of a large electric field in that region. This can have two effects, both of which would lead to a diode-like breakdown current. One is to drive the disproportionation of Ru^{2+} to Ru^{3+} and Ru^{1+} in the boundary region, and the other is to cause the migration of PF_6^- counterions in that zone. The latter effect would cause the degradation of the frozen gradient structure[74] through the electrolytic production of Ru^{2+} states outward from the boundary region (Figure 7, lower). The results in Figure 6 indicate that the latter process does occur under the conditions of these measurements. Since the mixed ionic/electronic current continues to separate rather than combine Ru^{3+} and Ru^{1+} states, there is no light emission. A crude estimate of the extent of the disturbance to the gradients in the boundary region under reverse bias can be made by assuming that all of the reverse bias current flow is electrolytic in nature. Integration of the reverse-bias current shown in Figure 4A indicates an electrolysis of 0.6 mol % of the film during the scan. This corresponds to the production of an all-Ru^{2+} boundary layer which is *ca*. 30 nm wide.

The extent to which large reverse-bias potentials also involve disproportionation of Ru^{2+} states within the boundary region is not clear. This highly endothermic reaction would require accumulation of a very large electrical field, but at the same time is aided by the rapid removal of Ru^{3+} and Ru^{1+} states from the boundary region. This is an important issue since if disproportionation does not occur, then breakdown of diode-like behavior under reverse bias voltage is only a signal of ionic motion which degrades the frozen gradient structure.

The "diode-like" light-emitting behavior observed here contrasts with that observed in a recent report in which a blend of a semiconducting luminescent polymer and an ionically conducting polymer (i.e. poly(ethylene oxide)) was used to form a light-emitting electrochemical cell.[75] The blend was sandwiched between two metal contacts and p- and n-doped regions electrolytically formed within the blend. Light emission occurred at the p−n junction between the two regions. Since the polymer blend was ionically conductive, the p- and n-doped regions became exchanged through a reversal of the voltage polarity across the metal contacts and diode-like behavior was not observed. In addition, the response time of the blend to a change in voltage polarity was a function of the blend's ionic mobility, necessitating addition of poly(ethylene oxide) in order to achieve ca. 1 s response times. In the present study removal of ionic conductivity yields much quicker response times and the achievement of diode-like behavior.

Conclusion

This study has demonstrated a *unique* form of light-emitting diode-like behavior. The basic mechanism by which the current−voltage diode-like behavior is expressed should be operant in any redox film with two (or more) serial mixed valent layers containing frozen concentration gradients. This prediction invites exploration of a broader range of chemical systems which is being done.

The poly$[Ru(vbpy)_3](PF_6)_2$ films used here, however, possess a number of limitations which would prohibit their use in practical devices. First, although the light-emitting diode-like behavior exhibits reasonable long-term stability, this stability is limited by the stability of the frozen gradient microstructure which is degraded under application of reverse-bias voltages through the onset of counterion movement in the film. This limitation potentially could be removed through study of other redox polymer systems that contain less mobile counterions. For light emission, a second important limitation is the low light levels observed, which are not visible to the naked eye.[76] The quantum efficiency is low and the overall level of light intensity is limited by the low conductivity of the film. This limitation could be addressed through the use of light-emitting redox polymer systems which possess higher conductivities and contain redox transition metal complexes which possess higher quantum yields for emission. It should be noted, however, that the use of low work function metal contacts which improve the performance of electroluminescent films,[38,39,42−44] should not affect the current or light-emission properties of the redox film employed here since electron transfers from inert metal electrodes to most redox polymers are facile and the locus of the diode-like property is remote from the electrode/polymer interfaces. Finally, the sample-to-sample variability of diode-like efficiency, presumably due to variability in film formation, should be addressable by improved synthetic schemes.

Acknowledgment. James Gardner is acknowledged for synthesis of the $[Ru(vbpy)_3](PF_6)_2$ monomer sample employed. This research was supported by grants from the National Science Foundation and Department of Energy.

JA953185W

(74) Although the mobility of the PF_6^- ions has been reduced by drying and cooling to 0 °C, in the presence of large electric fields, movement of these ions will be noticeable. At 0 °C the ionic conductance due to movement of the PF_6^- ions in the dry film was determined to be 1.32×10^{-10} A/V through the application of a ±200 mV potential scan across a dry all Ru^{2+} film at 300 mV /s.

(75) Pei, Q.; Yu, G.; Zhang, C.; Yang, Y.; Heeger, A. J. *Science* **1995**, *269*, 1086−1088. Pei, Q.; Yang, Y.; Yu, G.; Zhang, C.; Heeger, A. J. *J. Am. Chem. Soc.* **1996**, *118*, 3922−3929.

(76) The light output per unit area from a concentration gradient containing poly$[Ru(vbpy)_3](PF_6)_2$ film at 0 °C can be estimated to be 7.24×10^{10} photons/(cm²•s) for an applied voltage of 2.6 V. This estimate was made through a consideration of the film conductivity at 0 °C as obtained from Figure 5, along with the ECL efficiency and the total surface area of the IDA electrode (both gaps and fingers).